DOI:10.1021/jf9043937

JOURNAL OF AGRICULTURAL AND FOOD CHEMISTRY
ARTICLE

Thermal Degradation Kinetics of Chlorophyll Pigments in Virgin Olive Oils. 1. Compounds of Series *a*

Ramón Aparicio-Ruiz, Maria Isabel Mínguez-Mosquera, and Beatriz Gandul-Rojas*

Chemistry and Biochemistry Pigment Group, Department of Food Biotechnology, Instituto de la Grasa, CSIC, Avenida Padre García Tejero 4, 41012 Sevilla, Spain

Virgin olive oils (VOO) collected at three maturation stages were thermodegraded to determine the degradation kinetics of series *a* chlorophyll pigments. The proposed degradation mechanism involves reactions that alter the structure of the isocyclic ring of pheophytin, originating intermediary products such as pyropheophytin, 13^2-OH-pheophytin, and 15^1-OH-lactone-pheophytin, and reactions that affect the porphyrin ring, producing colorless compounds. The marked effect of temperature has been pointed out in these competitive processes with the formation of pyropheophytin and the significantly higher value of its kinetic constant. No significant effect of the oily medium on the reaction mechanisms of pyropheophytin and 15^1-OH-lactone-pheophytin has been found, comparing kinetic and thermodynamic parameters determined in the three VOO matrices of different pigment contents (high, medium, and low). The reaction mechanism of 13^2-OH-pheophytin, by contrast, was affected by the medium; the reaction rate was the same for all of the matrices only at the isokinetic temperature (51 °C).

KEYWORDS: Virgin olive oil; chlorophylls; pyropheophytin; thermodegradation; kinetics; Arrhenius parameters; isokinetic effect

INTRODUCTION

Chlorophyll pigments are responsible for the green color of plants and foodstuffs of vegetable origin. The chromatic properties of the chlorophylls have meant that for a long time their presence in foods was valued almost exclusively for this aesthetic function. Thus, research efforts in this field have primarily been aimed at optimizing the food-processing conditions to prevent or minimize the reaction of pheophytinization of the chlorophylls. This occurs under acid conditions and results in the color changing from bright green to olive green, which is not very attractive to the consumer (*1*).

Recent research has shown that the chlorophylls and their derivatives are somewhat more than color in food technology. As they are widespread in vegetable diets directly related with the attenuation of certain degenerative diseases, research on their bioactivity has gained importance, and it has been demonstrated that they have biological properties consistent with cancer prevention, such as antioxidant and antimutagenic activities, action modulating the activity of xenobiotic enzymes, and the induction of apoptotic events in cancer cell lines (*2*). Besides having these biological properties, the transformation of chlorophylls during fruit ripening and in the technological processing to obtain a food makes them authentic quality markers for the final product and potential traceability markers (*3*). Consequently, the characterization of both the content and type of pigments in the fresh vegetable material and of the transformations associated with a specific processing system will provide valuable information about the suitability of a process and about alterations, adulterations, or fraudulent manipulations.

The various technological alternatives for obtaining and/or preserving foods can affect differently the type and proportion of chlorophyll derivatives formed. In green oils of plant origin, the most widespread reaction is pheophytinization, resulting from a generalized liberation of acids following the mechanical breakdown of the plant tissue. The major pigment in this product is pheophytin *a* (**Figure 1**), with slight differences depending on whether the oil has been extracted by physical procedures, as in the case of olive oil (*4*), or chemical ones, using a solvent, as in the case of rapeseed oil, soybean oil, etc. (*5*). The processing conditions can also promote the activity of hydrolytic endogenous enzymes such as chlorophyllase and/or oxidative ones (peroxidase, lipoxygenase, etc.), so that dephytylated chlorophyll derivatives, mainly pheophorbide *a*, and oxidized ones, such as 13^2-OH-pheophytin *a* and 15^1-OH-lactone pheophytin *a*, can be found in the oil (*3*, *6*). The oil storage conditions are also factors to be considered. In the light, the predominant reaction is the cleavage of the chromophore of pheophytin by photo-oxidation (*7*), whereas in the dark the reactions of pheophytinization and allomerization take place, and another oxidative reaction, decarbomethoxylation on C-13^2, develops slowly, originating pyropheophytin (**Figure 1**) (*5*, *8*). This reaction becomes the main one in the heat treatments for deodorizing vegetable oils (*9*, *10*) and has led to investigating the possibilities this pigment offers as a marker of quality and traceability in virgin olive oil (*3*, *8*, *11*).

*Corresponding author (telephone 34-954691054; fax 34-954691262; e-mail gandul@cica.es).

 Published on Web 04/28/2010

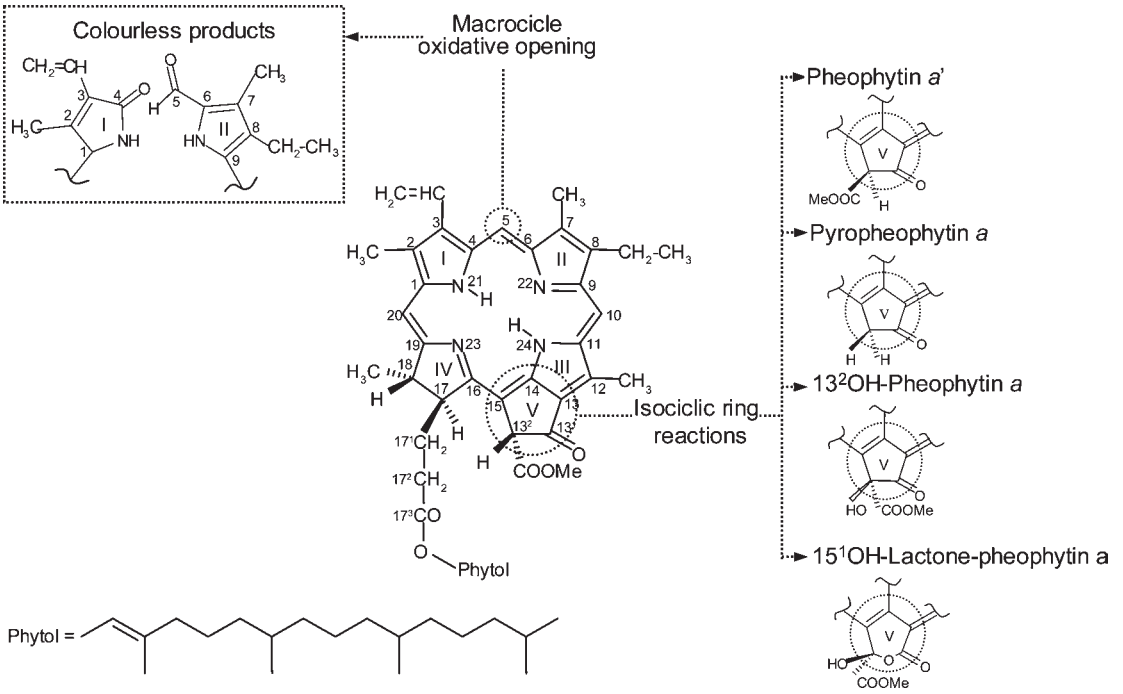

Figure 1. Structures of pheophytin *a* and derivative compounds.

Virgin olive oil (VOO) is obtained from the fruit of the olive only by physical procedures under conditions, in particular with regard to heat, that do not involve alteration of the oil (*12*). Although a recently extracted VOO does not contain pyropheophytin *a*, this compound is generated during storage, the amount depending on the initial content of pheophytin *a* and the conditions to which the oil has been exposed during storage.

It would therefore be of interest to construct a mathematical model enabling a reasonably accurate prediction of the amount of pyropheophytin *a* that a VOO might have during a specific period of storage and under specific conditions of a prefixed mean temperature. The value obtained would establish whether the actual amount of pyropheophytin *a* measured in an olive oil marketed as "virgin" corresponds with proper storage conditions or, in contrast, is the result of the fraudulent addition of an oil with some organoleptic defect that has been deodorized (the so-called "deodorato oil").

This research work is aimed at the kinetic study and characterization of the thermodynamic parameters governing the thermodegradation reactions of series *a* chlorophyll pigments in VOO to establish future mathematical models enabling the prediction of the formation or degradation of such pigments during VOO storage.

MATERIALS AND METHODS

Chemicals and Standards. Tetrabutylammonium acetate and ammonium acetate were supplied by Fluka (Zwijndrecht, TheNetherlands). HPLC reagent grade solvents were purchased from Teknokroma (Barcelona, Spain), and analytical grade solvents were supplied by Panreac (Barcelona, Spain). For the preparation, isolation, and purification of chlorophyll pigments, analytical grade reagents were used (Panreac). The deionized water used was obtained from a Milli-Q 50 system (Millipore Corp., Bedford, MA). Standards of chlorophyll *a* (chl*a*) were supplied by Sigma-Aldrich Co. Standards of pheophytin *a* (phy*a*) and pyropheophytin *a* (pyphy*a*) were provided by Wako Chemicals GmbH (Neuss, Germany). The C-13 epimer of phy*a* was prepared by treatment with chloroform according to the method of Watanabe et al. (*13*). 13^2-OH-phy*a* was obtained by selenium dioxide oxidation of phy*a* at reflux heating for 4 h in pyridine solution under argon (*14*). 15^1-OH-lactone-phy*a* was obtained from phy*a* by alkaline oxidation in aqueous media according to the method of Mínguez-Mosquera and Gandul-Rojas (*15*).

Samples. The study of thermal degradation of pigments was carried out with virgin olive oils obtained from a single industrial mill (Cooperativa Sor Ángela de la Cruz, Estepa, Seville) to avoid any effect of pedoclimatic and agricultural parameters and the industrial variables of the extraction systems in the comparative studies. To have three lots of oil with a differing pigment content, the starting material used was a mixture of two oil variety olives, Hojiblanca and Manzanilla, picked in three different months: November (sample N), December (sample D), and January (sample J). The proportions of fruits between varieties were 20:80, 80:20, and 100:0, respectively. The dates of picking correspond to high, medium, and low pigment levels (referring to the green color) and correlated inversely with the degree of fruit ripening according to the method of Walalí-Loudiyi et al. (*16*).

Heat Treatment. Preliminary assays, with a commercial sample of VOO, enabled an approximate determination of the degree of conversion for the main reactions to be studied and established a range of times for an appropriate sampling at each temperature. The total time of each experiment changed depending on the assay temperature: 42 h (120 °C), 64 h (100 °C), 370 h (80 °C), and 744 h (60 °C). At least 128 aliquots (32 for each of the four assay temperatures) were separated from each oil lot (samples N, D, and J). These aliquots were put into glass tubes that were sealed in the absence of air and placed in thermostated ovens at the temperatures fixed for each experiment. These four temperatures were used to determine the kinetic and thermodynamic parameters (reaction order, reaction rate, and activation energies).

For each oil lot, two samples were analyzed for each time/temperature pair. The samples were removed from the thermostated ovens at fixed time intervals, depending on each experiment, to obtain a total of at least 16 duplicate samples. The samples were cooled rapidly in an ice bath and then kept at −20 °C until analysis of the pigments.

Extraction and Analysis of Chlorophyll Pigments. All procedures were performed under green lighting to avoid any photo-oxidation of chlorophyll compounds. Pigment extraction was performed by liquid-phase distribution. This method was developed for virgin olive oil by Mínguez-Mosquera et al. (*4*). The technique is based on the selective separation of components between *N*,*N*-dimethylformamide (DMF) and hexane. The oil sample (10−15 g) was dissolved directly in 150 mL of DMF and treated with five 50 mL successive portions of hexane in a decanting funnel. The hexane phase carried over lipids and carotene fraction, whereas the DMF phase retained chlorophyll pigments and

xanthophylls. This system yielded a concentrated pigment solution that was oil free and could be adequately analyzed by chromatographic techniques.

HPLC analysis of chlorophyll pigments was performed according to the method described by Mínguez-Mosquera et al. (*17*), using a reverse-phase column (20 cm × 0.46 cm) packed with 3 μm C18 Spherisorb ODS2 (Teknokroma, Barcelona, Spain) and an elution gradient with the solvents (A) water/ion-pair reagent/methanol (1:1:8, v/v/v) and (B) acetone/methanol (1:1 v/v), at a flow rate of 1.25 mL/min. The ion-pair reagent was 0.05 M tetrabutylammonium acetate and 1 M ammonium acetate in water. The pigments were identified by cochromatography with the corresponding standard and from their spectral characteristics described in detail in previous papers (*17*, *18*). The online UV−vis spectra were recorded from 350 to 800 nm with the photodiode array detector. Pigments were quantified at the wavelength of maximum absorption (410 nm for phy*a*, 13^2-OH-phy*a*, and pyphy*a* and 400 nm for 15^1-OH lactone-phy*a*) and were quantified from the corresponding calibration curves (amount versus integrated peak area). The calibration equations were obtained by least-squares linear regression analysis over a concentration range according to the levels of these pigments in VOO. Injections in duplicate were made for five different volumes at each standard solution.

Kinetic Parameters. Changes in experimental data of pigment concentration, expressed in micromoles per kilogram, were used to calculate kinetic parameters by least-squares nonlinear regression analysis. The reaction order (n) and rate constant (k) were determined by trial and error using the integral method: a reaction order is initially assumed in the rate equation and then is integrated to obtain a mathematical expression that relates pigment concentration (C) with time (t). The mathematical expression that best fits the changes in the experimental data with the reaction time was selected to verify the order (assumed ad initio) and used to obtain the rate constant (k).

Thermodynamic Parameters. The effect of temperature on the rate constant was evaluated by means of the Arrhenius equation with a simple reparametrization (*19*) by using a reference temperature T_{ref}

$$k = k_{ref} \times \exp\left[\frac{-E_a}{R}\left(\frac{1}{T}-\frac{1}{T_{ref}}\right)\right]$$

where R is the molar gas constant (1.98 cal mol^{-1} K^{-1}), T is the absolute temperature (K), E_a is the activation energy (cal mol^{-1}), k is the specific reaction rate constant at the temperature T, and k_{ref} is the specific reaction rate constant at the reference temperature T_{ref}. The reference temperature should preferably be chosen in the middle of the studied temperature regimen. Therefore, E_a was estimated on the basis of nonlinear regression analysis of k_i versus $1/T_{ij}$ (i = N, D, J; j = 60, 80, 100, 120 °C).

According to activate complex theory, enthalpy ($\Delta H^{\ddagger}$) and entropy ($\Delta S^{\ddagger}$) of activation were determined by using the Eyring eq 1

$$\ln(k/T) = \frac{-\Delta H^{\ddagger}}{RT} + \frac{\Delta S^{\ddagger}}{R} + \ln\left(\frac{k_b}{h}\right) \quad (1)$$

where k is the rate constant at temperature T, k_b is the Boltzmann constant, R is the molar gas constant, and h is the Planck constant.

Therefore, $\Delta H^{\ddagger}$ and $\Delta S^{\ddagger}$ were estimated on the basis of linear regression analysis of $\ln(k_i/T_{ij})$ versus $1/T_{ij}$. The Gibbs free energy was estimated according to the Gibbs equation:

$$\Delta G^{\ddagger} = \Delta H^{\ddagger} - T\Delta S^{\ddagger}$$

The pairs of $\Delta H^{\ddagger}$ and $\Delta S^{\ddagger}$ obtained were linearly correlated using the last equation, from which the isokinetic temperature (T_{isok}) and its corresponding Gibbs free energy (AG_{isok}) for the reaction could be estimated.

Calculations and Statistical Data Analysis. Estimated parameters were expressed as means ± SE and were analyzed for differences between means using one-way analysis of variance (ANOVA). The Brown and Forsythe test (*20*) was used as a post hoc comparison of statistical significance (p values < 0.05). Least-squares and nonlinear regression analysis were performed using Statistica 6.0 (StatSoft, Inc., 2001) and Statgraphics Centurion XV for Windows (Statpoint Technologies, Inc., 2005).

Table 1. Initial Content for Chlorophyll Compounds of Series *a* in Virgin Olive Oils[a]

sample[b]	phy	OH-phy	lac-phy	pyphy	total
N	15.67 ± 0.23	0.26 ± 0.00	0.31 ± 0.00	0.24 ± 0.00	16.45 ± 0.21
D	8.57 ± 0.34	0.20 ± 0.00	0.28 ± 0.00	0.10 ± 0.00	9.15 ± 0.33
J	2.96 ± 0.11	0.08 ± 0.00	0.14 ± 0.00	0.02 ± 0.00	3.19 ± 0.11

[a] Data, expressed as μmol/kg, represent mean values ± SD for three determinations. [b] The sample codes correspond to the harvesting date of the olive fruits used to obtain the virgin olive oils studied: November (N), December (D), January (J).

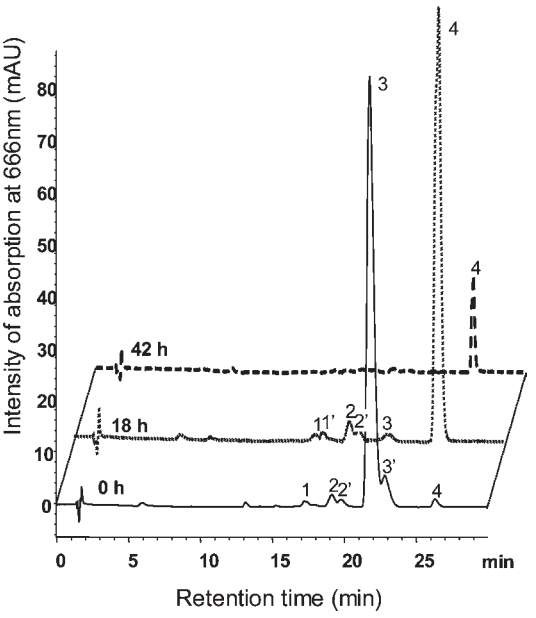

Figure 2. HPLC chromatograms of chlorophyll pigments from virgin olive oils (sample N), at initial time (0 h) and after 18 and 42 h of thermal treatment at 120 °C. Detection was by absorption at 666 nm. Peaks: 1, lac-phy*a*; 1′, lac-phy*a*′; 2, OH-phy*a*; 2′, OH-phy*a*′; 3, phy*a*; 3′, phy*a*′; 4, pyphy*a*.

RESULTS AND DISCUSSION

Kinetic Study of Series *a* Chlorophyll Compounds. Table 1 shows the initial content of series *a* chlorophyll pigments in the studied VOO matrices of high (N), medium (D), and low (J) pigmentation. The qualitative pigment profile is that typical of a virgin olive oil (*3*, *6*). Phy*a* is the major chlorophyll derivative, with a minimal percentage of allomerized derivatives (OH-phy*a* and lac-phy*a*) and pyphy*a* being detected.

Quantitatively, the total content of series *a* chlorophyll compounds for each matrix is a reflection of the differences required in the starting samples to enable studying the effect of the pigment composition of the VOO matrix on the kinetics of thermal degradation of the chlorophyll compounds.

Figure 2 shows typical HPLC chromatograms of an olive oil pigment extract at three significant moments of the thermal degradation process studied: initial sample and after 18 and 42 h of heating at 120 °C. The changes in the main chlorophyll pigments with heating time are those expected from the bibliography for other food matrices. As the concentration of the phy*a* and phy*a*′ (peaks 3 and 3′) gradually falls, three compounds of oxidative degradation are detected: pyphy*a* (peak 4); OH-phy*a* and OH-phy*a*′ (peaks 2 and 2′); and lac-phy*a* and lac-phy*a*′ (peaks 1 and 1′). Dephytylated chlorophyll derivatives were not detected. The content of these oxidized pigments increased gradually from time zero until intermediate stages of the heat treatment and then began to fall, in some cases disappearing in the

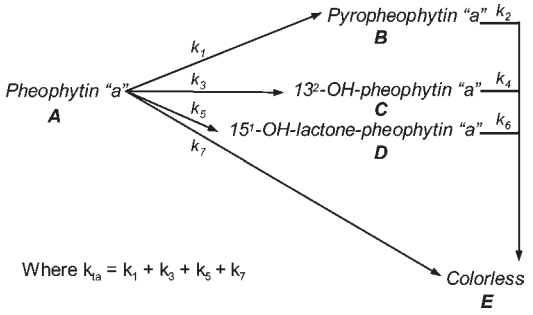

Figure 3. Kinetic mechanisms for thermodegradation pathway of pheophytin *a* in virgin olive oil.

final phase of heat treatment. No other colored degradation compound was detected as being formed in their place.

In accord with the results of qualitative and quantitative changes in pigments, the reaction mechanism proposed for the series *a* compounds is shown in **Figure 3**. It encompasses two different types of oxidative reaction. The first reactions affect the isocyclic ring (**Figure 1**) and produce the formation of pyphy*a* (by loss of the carbomethoxide group of pheophytin), OH-phy*a* (by hydroxylation at C-13^2), and lac-phy*a* (by formation of a lactone ring). The second type of reaction affects the porphyrin ring, causing its oxidative opening and originating colorless products both from the intermediary degradation products and directly from pheophytin *a*. In contrast to the general mechanism of chlorophyll pigment degradation proposed by Marangoni (*21*) for green tissues, the mechanism proposed here does not include the formation of pheophorbide from pheophytin. Independently of the fact that an enzymatic de-esterification of the phytol by chlorophyllase, as occurs in fruits and green tissues (*22*), can be ruled out a priori in an oily matrix, neither has any type of chemical de-esterification been detected.

In accord with the mechanism proposed, this total degradation assumes a series of parallel and consecutive reactions, illustrated in **Figure 3**. The corresponding kinetic equations are expressed as

$$V_{\text{phy}a} = -\frac{\mathrm{d}[\mathrm{A}]}{\mathrm{d}t} = k_{t_a}[\mathrm{A}]^n;\ k_{t_a} = k_1 + k_3 + k_5 + k_7 \qquad (2)$$

$$V_{\text{pyphy}a} = \frac{\mathrm{d}[\mathrm{B}]}{\mathrm{d}t} = k_1[\mathrm{A}]^n - k_2[\mathrm{B}]^n \qquad (3)$$

$$V_{\text{OH-phy}a} = \frac{\mathrm{d}[\mathrm{C}]}{\mathrm{d}t} = k_3[\mathrm{A}]^n - k_4[\mathrm{C}]^n \qquad (4)$$

$$V_{\text{lac-phy}a} = \frac{\mathrm{d}[\mathrm{D}]}{\mathrm{d}t} = k_5[\mathrm{A}]^n - k_6[\mathrm{D}]^n \qquad (5)$$

$$V_{\text{nc}} = \frac{\mathrm{d}[\mathrm{E}]}{\mathrm{d}t} = k_7[\mathrm{A}]^n + k_2[\mathrm{B}]^n + k_4[\mathrm{C}]^n + k_6[\mathrm{D}]^n \qquad (6)$$

where [A] is the concentration of phy*a*, [B] is the concentration of pyphy*a*, [C] is the concentration of OH-phy*a*, [D] is the concentration of lac-phy*a*, and [E] is the concentration of noncolored products (nc); $k_1, k_2, k_3, k_4, k_5, k_6$, and k_7 are the rate constants for the different reactions; and n is the reaction order.

From the balance of material of all the species, eq 7, the concentration of colorless compounds with time is obtained:

$$[\mathrm{A}]_0 + [\mathrm{B}]_0 + [\mathrm{C}]_0 + [\mathrm{D}]_0 + [\mathrm{E}]_0 = [\mathrm{A}] + [\mathrm{B}] + [\mathrm{C}] + [\mathrm{D}] + [\mathrm{E}] \qquad (7)$$

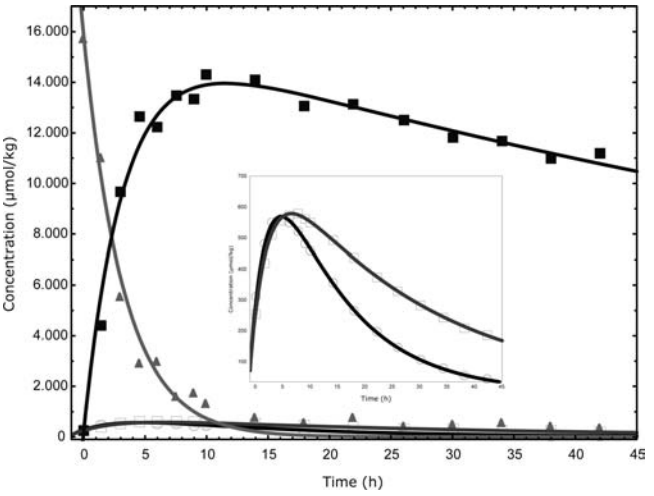

Figure 4. Evolution of concentration−time of pheophytin *a* (▲), pyropheophytin *a* (■), 13^2-OH-pheophytin *a* (□), and 15^1-OH-lactone-pheophytin *a* (○) in virgin olive oil (sample N) during 42 h at 120 °C and corresponding fits (—) to the mathematical model developed in this study (eqs 8−11).

Here $[\mathrm{A}]_0$ is the initial concentration of phy*a*, $[\mathrm{B}]_0$ is the initial concentration of pyphy*a*, $[\mathrm{C}]_0$ is the initial concentration of OH-phy*a*, $[\mathrm{D}]_0$ is the initial concentration of lac-phy*a*, $[\mathrm{E}]_0$ is the initial concentration of nc, and the concentrations [A]−[E] are those described for eqs 2−6.

Resolving the kinetic mechanism, assuming an order of 1 ($n = 1$) and that all of the reactions are irreversible, we get

$$[\mathrm{A}] = [\mathrm{A}]_0\, \mathrm{e}^{-k_{t_a}\cdot t} \qquad (8)$$

$$[\mathrm{B}] = \frac{k_1[\mathrm{A}]_0}{k_2 - k_{t_a}}[\mathrm{e}^{-k_{t_a}\cdot t} - \mathrm{e}^{-k_2\cdot t}] + [\mathrm{B}]_0\, \mathrm{e}^{-k_2\cdot t} \qquad (9)$$

$$[\mathrm{C}] = \frac{k_3[\mathrm{A}]_0}{k_4 - k_{t_a}}[\mathrm{e}^{-k_{t_a}\cdot t} - \mathrm{e}^{-k_4\cdot t}] + [\mathrm{C}]_0\, \mathrm{e}^{-k_4\cdot t} \qquad (10)$$

$$[\mathrm{D}] = \frac{k_5[\mathrm{A}]_0}{k_6 - k_{t_a}}[\mathrm{e}^{-k_{t_a}\cdot t} - \mathrm{e}^{-k_6\cdot t}] + [\mathrm{D}]_0\, \mathrm{e}^{-k_6\cdot t} \qquad (11)$$

In accord with the proposed kinetic eqs 8−11 and by nonlinear regression analysis of the experimental data, the rate constants for each of the proposed reactions in the mechanism (**Figure 3**) were estimated. **Figure 4** exemplifies, for the treatment at 120 °C of the high-pigmentation matrix (sample N), the concentration changes found and the regressions estimated. **Table 2** shows the values for the estimated rate constant, together with their standard error, and the determination coefficient (R^2) for each reaction studied.

The determination coefficients obtained indicate a good fit of the experimental data to the equations proposed and demonstrate that the first-order mechanism is appropriate for describing the thermal degradation of the series *a* chlorophyll compounds in the VOO. The first-order kinetics model has also been reported for chlorophyll degradation during the fermentation processing of food matrices such as pickles, olives, and coleslaw (*23*, *24*) and in the heat treatment of spinach puree (*25*).

The results demonstrate a marked effect of temperature in all of the reactions, both parallel and consecutive, that compete in the mechanism and which have phy*a* as the original compound. Of these reactions, that of pyphy*a* formation presents significantly higher kinetic constants over the whole temperature range.

Table 2. Rate Constants (k) and Determination Coefficients (R^2) Estimated for the Kinetic Mechanism of the Thermal Degradation of Pheophytin *a* in VOO

		120 °C			100 °C			80 °C			60 °C		
reaction[a]	sample[b]	$k^c \times 10^3(h^{-1})$	SE	R^2	$k^c \times 10^3(h^{-1})$	SE	R^2	$k^c \times 10^3(h^{-1})$	SE	R^2	$k^c \times 10^3(h^{-1})$	SE	R^2
D. phy*a*	N	312.10 a	16.44	0.98	105.58 a	4.56	0.98	22.90 a	1.09	0.99	2.87 a	0.16	0.96
k_{ta}	D	176.60 b	8.16	0.98	93.22 b	4.80	0.98	17.48 b	1.26	0.96	1.89 b	0.09	0.97
	J	185.10 b	12.33	0.96	79.49 c	5.19	0.96	16.57 b	1.26	0.97	2.3 8 c	0.18	0.94
F. pyphy*a*	N	299.82 a	5.81	0.98	103.96 a	2.25	0.97	22.62 a	0.54	0.98	2.27 c	0.08	0.98
k_1	D	175.14 b	5.05	0.97	93.20 b	2.41	0.97	15.33 b	0.68	0.93	1.15 d	0.04	0.99
	J	187.88 b	9.80	0.98	68.25 d	3.23	0.93	17.20 c	0.71	0.96	1.81 b	0.05	0.99
F. OH-phy*a*	N	9.75 c	0.03	1.00	3.29 e	0.03	1.00	1.37 d	0.05	0.92	0.33 e	0.01	0.98
k_3	D	4.20 d	0.06	0.99	2.75 f	0.03	0.99	1.16 e	0.00	1.00	0.31 f	0.00	1.00
	J	3.68 e	0.07	0.98	2.45 g	0.03	1.00	0.83 f	0.02	0.99	0.25 g	0.00	1.00
F. lac-phy*a*	N	11.90 f	0.26	0.99	1.24 h	0.03	0.97	0.42 g	0.01	0.98	0.28 h	0.01	0.96
k_5	D	3.39 g	0.09	1.00	0.82 i	0.03	0.93	0.39 h	0.00	1.00	0.21 i	0.00	1.00
	J	4.87 h	0.21	0.99	0.73 j	0.03	0.93	0.24 i	0.01	0.95	0.15 j	0.00	1.00
D. pyphy*a*	N	9.68 c	1.17	0.98	3.10 k,e−g	0.72	0.97	1.12 j,d−f	0.18	0.98	0.23 k,e-j	0.11	0.98
k_2	D	8.77 c	1.69	0.97	3.48 k,e−g	0.84	0.97	1.27 j,d,e	0.31	0.93	0.19 k,e-j	0.10	0.99
	J	13.22 i,j	1.79	0.98	1.15 k,e−g	1.57	0.93	0.93 j,e,m	0.27	0.96	0.23 k,j	0.08	0.99
D. OH-phy*a*	N	35.22 k	0.18	1.00	12.36 l	0.21	1.00	1.42 k,d,e	0.22	0.92	0.31 l,e-i	0.09	0.98
k_4	D	19.59 i	0.45	0.99	13.57 m	0.24	0.99	1.15 k,e	0.02	1.00	0.36 l,e,f	0.04	1.00
	J	15.41 j	0.55	0.98	12.51 l	0.20	1.00	0.76 l,f	0.06	0.99	0.40 l,m	0.02	1.00
D. lac-phy*a*	N	78.32 l	2.20	0.99	3.77 o,w,y	0.24	0.97	0.63 m	0.07	0.98	0.42 m,e-h	0.11	0.96
k_6	D	56.74 m	1.03	1.00	1.96 o,w,y	0.20	0.93	0.55 m	0.02	1.00	0.21 n,h-j	0.05	1.00
	J	45.30 n	1.53	0.99	2.54 o,g,f	0.16	0.93	0.37 n,g,h	0.05	0.95	0.24 n,g-i	0.03	1.00

[a] Reactions according to the kinetic mechanism shown in **Figure 3**: D, degradation; F, formation; Phy, pheophytin; pyphy, pyropheophytin; OH-phy, 13^2-OH-pheophytin; lac-phy, 15^1-OH-lactone-pheophytin. [b] Sample code as in **Table 1**. [c] Values are obtained from a minimum of 16 experimental data points analyzed in duplicate. SE, standard error. At each temperature, different letters between rows indicate significant differences ($p \leq 0.05$).

For each matrix, the overall degradation rate of phy*a* increases markedly with temperature, particularly in the highly pigmented matrix N, where k at 60 °C is smaller by factors of approximately 8, 35, and 100 than at 80, 100, and 120 °C, respectively. The marked effect of temperature on the degradation of chlorophylls has been demonstrated in green tissues (*25*) and broccoli juice (*26*), where in general the reaction rate doubles for each 10 °C increase in temperature. The kinetic constants for each individual reaction of formation and degradation of pyphy*a*, OH-phy*a*, and lac-phy*a* are also clearly dependent on the temperature, above all for pyphy*a*. The differences are less marked at the lowest temperatures (60 and 80 °C).

With regard to the type of reaction, the rate of pyphy*a* formation is significantly very much higher than that of the other reactions of formation, for all of the temperatures and matrices studied.

This result is not surprising because their different reaction mechanisms are well-known. The allomerization reactions (OH-phy*a* and lac-phy*a* formation) have shown a mechanism via free radicals (*14*) in which oxygen availability is a critical factor (*8*, *11*). The experimental conditions of this study, in which the samples were sealed in the absence of air, promote pyropheophytination reaction against allomerization reaction. The reactions of degradation to colorless compounds that involve cleavage and destruction of the chlorine macrocycle are not prevalent in the experimental conditions of darkness. However, these reactions are prevalent under light exposure, when chlorophyll pigments are photo-oxygenated by singlet oxygen (*7*) through a self-destruction mechanism of porphyrins due to its photosensitizing capability (*14*).

The differences found in the kinetic constants, depending on the starting material (initial composition of the matrix), indicate that the matrices could be considered a priori different reaction media, in which triacylglycerols and minor compounds with antioxidant activity, such as polyphenols, tocopherols, carotenoids, can modulate the degradation reactions (*27*).

For all of the temperatures, the k of total degradation of phy*a* is always higher ($p < 0.05$) in sample N than in the other two (samples D and J), which in some 50% of cases do not present significant differences between them. This implies a greater lability of the matrix N to the degradation of phy*a*. Similar deductions can be made regarding the reaction of pyphy*a* formation, where the matrix N shows the highest values of k at all temperatures; however, in this case some 75% of the data present differences of rate constants at each temperature.

This also occurs for the reactions of formation of OH-phy*a* and lac-phy*a*, although the differences are less marked, and in all cases there are significant differences in the rate constant between the oily matrices.

If we compare for each chlorophyll derivative the rate constant of the formation reaction with that of the degradation reaction, it is observed that for pyphy*a* the k of formation is some 10−30 times higher than that of degradation, in the temperature range studied. In contrast, for the compounds OH-phy*a* and lac-phy*a*, the k of degradation is higher than that of formation at the highest temperatures (100 and 120 °C) and does not present significant differences at the lowest temperatures (60 and 80 °C).

A total of seven kinetic constants are obtained for each sample (three) and temperature (four) studied. According to the kinetic mechanism (**Figure 3**), the sum of constants k_1, k_3, k_5, and k_7 should be equal to k_{ta} (kinetic constant of the total degradation of phy*a*). From the corresponding calculations (**Table 3**), it can be seen that, except in 17% of the experiments (two cases), the

sum of the constants k_1, k_3, and k_5 does not differ significantly ($p \leq 0.05$) from k_{ta}. This result allows ignoring k_7, that is, ruling out the hypothesis in the kinetic mechanism that noncolored products are formed from pheophytin *a*.

Thermodynamic Study. Table 4 displays the values obtained for the thermodynamic parameters (entropy, enthalpy, activation energy, pre-exponential factor, and Gibbs free energy), with their respective standard errors, in the total degradation of phy*a*, the formation of the products pyphy*a*, OH-phy*a*, and lac-phy*a*, and the degradation of these to noncolored products. The values for the parameters are deduced from the equations described under Thermodynamic Parameters.

Table 3. Analysis of Variance between the Rate Constant for the Total Degradation of Pheophytin *a* (k_{ta}) and the Sum of the Rate Constants for the Individual Formation Reactions, Pyphy (k_1), OH-phy (k_3), and Lac-phy (k_5) by *t* Test of Brown and Forsythe (*20*)

T (°C)	sample[a]	$(k_1 + k_3 + k_5) \times 10^3$ (h^{-1})	SE[b]	$(k_{ta}) \times 10^3$ (h^{-1})	SE
120	N	321.47	5.81	312.10	16.44
	D	182.74	5.05	176.60	8.16
	J	196.43	9.80	185.10	12.33
100	N	108.50	2.25	105.58	4.56
	D	96.77	2.41	93.22	4.80
	J	71.42	3.23	79.49	5.19
80	N[c]	24.41	0.54	22.90	1.09
	D	16.88	0.68	17.48	1.26
	J	18.26	0.71	16.57	1.26
60	N	2.87	0.09	2.87	0.16
	D[c]	1.67	0.04	1.89	0.09
	J	2.20	0.05	2.38	0.18

[a] Sample codes as in **Table 1**. [b] SE, standard error. [c] Significant differences ($p \leq 0.05$) between ($k_1 + k_3 + k_5$) and k_{ta}.

To study the effect of the type of matrix on the reaction mechanism, we compared the thermodynamic parameters obtained in the three lots of VOO of differing pigment contents. No significant difference was found in the parameters characterizing the reaction of pyphy*a* formation (*t* test $p \leq 0.05$), enabling all of the matrices to be considered a single reaction medium in this case. There was a slight effect of the matrix on the formation reactions of OH-phy*a* and lac-phy*a*.

With regard to the thermodynamic parameters of the Arrhenius equation (activation energy), there are significant differences between the three matrices (*t* test $p \leq 0.05$) for the reaction of OH-phy*a* formation.

The reactions of allomerization (OH-phy*a* and lac-phy*a* formation) and decoloration follow a free radical mechanism. It seems a logical way to find an effect of the matrix because of the presence of compounds as radical scavengers that can partially inhibit the mechanism. α-Tocopherol, β-carotene, and lutein have this capability, and they are present in VOO. Their highest content is at the beginning of the harvesting season (matrix N). However, the formation reaction of OH-phy*a* followed an opposite relationship; the higher the pigment content, the higher the energy of activation. Thus, a smaller increase in temperature is required to produce the formation of OH-phy*a* more quickly (**Table 4**). Psomiadou and Tsimidou (*28*) did not find a clear relationship between the content of radical scavengers and the formation of OH-phy in VOO stored in darkness. Further studies are required to clarify this point, under experimental conditions that favor these oxygen radical reactions.

From the theory of the activated complex, it is deduced that the energy requirement (E_a value) for pyphy*a* to achieve the structure

Table 4. Thermodynamic Parameters[a] for the Thermodegradation Reactions of Chlorophyll Compounds of Series *a* in Virgin Olive Oil

reaction[b]	sample[c]	$\Delta S^{\ddagger}$ [cal/(mol·K)]	SE[d]	$\Delta H^{\ddagger}$ [kcal/(mol)]	SE	E_a (kcal/mol)	SE	$\Delta G^{\ddagger}_{298}$ (kcal/mol)	SE
D. phy*a*	N	−26.96	1.93	19.69	0.70	20.43	0.23	27.72	0.70
	D	−28.55	3.70	19.36	1.34	19.89	0.63	27.87	1.34
	J	−31.07	2.32	18.44	0.84	19.02	0.37*[e]	27.70	0.84
F. pyphy*a*	N	−24.95	2.63	20.47	0.95	21.28	0.27	27.91	0.95
	D	−22.99	4.65	21.49	1.68	22.01	0.73	28.34	1.68
	J	−28.72	2.74	19.36	0.99	20.25	0.28*	27.92	0.99
F. OH-phy*a*	N	−49.38	1.04*	13.71	0.37*	14.72	0.08*	28.43	0.37
	D	−59.02	1.76	10.48	0.64	11.65	0.46*	28.07	0.64
	J	−57.32	1.69	11.22	0.61	7.47	1.50*	28.30	0.61
F. lac-phy*a*	N	−46.57	6.04	15.11	2.18	16.11	0.57	28.99	2.18
	D	−59.00	2.94*	10.97	1.06*	11.81	0.49*	28.56	1.06
	J	−50.62	4.75	14.11	1.71	14.91	0.53	29.19	1.71
D. pyphy*a*	N	−45.53	1.04	15.21	0.38	16.19	0.06*	28.78	0.38
	D	−44.37	4.65	15.64	1.68	16.69	0.23	28.87	1.68
	J	−30.92	2.74*	20.78	0.99*	17.39	0.53	30.00	0.99
D. OH-phy*a*	N	−28.96	2.30*	20.64	0.83*	20.65	0.26*	29.27	0.83
	D	−35.89	4.62	18.23	1.67	17.72	0.87	28.93	1.67
	J	−39.10	6.14	17.18	2.22	16.23	1.03	28.83	2.22
D. lac-phy*a*	N	−26.66	8.59	21.63	3.10	22.70	0.41	29.58	3.10
	D	−25.39	8.31	22.41	3.00	24.20	0.39*	29.98	3.00
	J	−27.03	8.15	21.86	2.94	22.62	0.39	29.92	2.94

[a] $\Delta S^{\ddagger}$, activation entropy; $\Delta H^{\ddagger}$, activation enthalpy; E_a, activation energy; $\Delta G^{\ddagger}$, Gibbs free energy. [b] Reactions according to the kinetic mechanism shown in **Figure 3**; D, degradation; F, formation; phy, pheophytin; pyphy, pyropheophytin; OH-phy, 13^2-OH-pheophytin; lac-phy, 15^1-OH-lactone-pheophytin. [c] Sample codes as in **Table 1**. [d] Standard error. [e] * indicates significant differences for a parameter between different samples ($p \leq 0.05$).

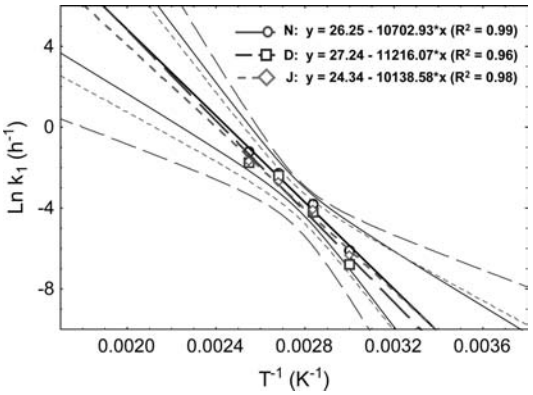

Figure 5. Arrhenius plot for the formation of pyropheophytin *a* in VOO samples studied (N, ○; D, □; J, ◇). Confidence intervals (95%).

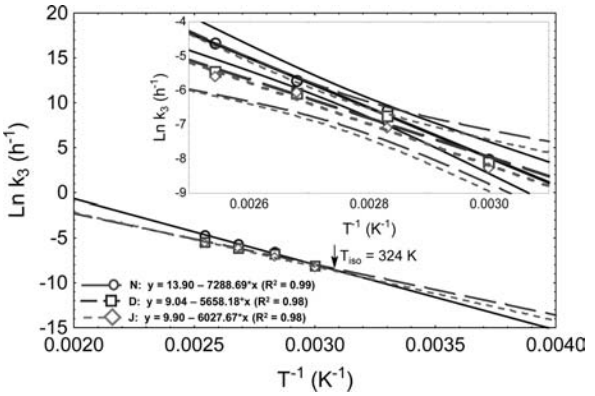

Figure 6. Arrhenius plot for the formation of 13^2-OH-pheophytin *a* in VOO samples studied (N, ○; D, □; J, ◇). Confidence intervals (95%).

of the activated complex in the formation reaction is slightly higher than those for lac-phy*a* and OH-phy*a*, and in that order.

In all cases the enthalpy values ($\Delta H^{\ddagger}$) are always positive, as are the Gibbs free energy values ($\Delta G^{\ddagger}$); in contrast, the values of $T\Delta S^{\ddagger}$ are always negative, making the reactions nonspontaneous.

Isokinetic Ratio. Various thermodynamic studies (*29*, *30*) determine the isokinetic ratio to differentiate groups of reactions that are apparently similar. Such reactions, grouped around a parameter that can have a physical or a chemical significance, may take place under different reaction mechanisms, or a particular step of the reaction may have particular importance. In the first case (changes of the reaction mechanism or variations in the structure of the activated complex) alterations would be produced in the values of the activation energy (*31*). In the second case (greater importance of some specific step of the mechanism) alterations would not be produced in the thermodynamic parameters, but there would be a selectivity of the reaction toward one of the reagents, differentiating that particular step (or steps) from the rest by the parameter around which they are grouped. Thus, a study of the isokinetic ratio can be an excellent work tool for determining whether there are changes in the reaction mechanism under different experimental conditions.

The isokinetic effect (or isoequilibrium) has to be defined as the existence of a point of intersection between the straight lines of Arrhenius (or van't Hoff) that describe the thermodynamics of a series of similar reactions or a reaction in different media (*32*). This cutoff point is the isokinetic temperature at which the reactions take place at identical rates. Specifically, the experiments performed deal with studying the same reaction taking place in different oily matrices. We thus find ourselves in the second case: a greater importance of a particular step of the mechanism. To study the existence of the isokinetic ratio between the oily matrices, the Arrhenius equation straight lines obtained for each of the three oily matrices studied were represented together. The study was repeated for each of the reactions comprising the mechanism of heat degradation of phy*a*; no isokinetic ratio was found for any of them, except in the reaction of OH-phy*a* formation.

For the case of the reaction of pyphy*a* formation (**Figure 5**), we could not conclude that there was an isokinetic ratio as the Arrhenius straight lines for the three samples (N, D, J) did not present any common cutoff point. These straight lines are almost parallel, but are also very close to one another (all the points lie within the same interval of confidence). They are, therefore, isoenthalpic and isoentropic straight lines. This observation is coherent with the thermodynamic parameters (**Table 4**), which do not show significant differences (*t* test $p \leq 0.05$) between the different oily matrices. Thus, there is no isokinetic ratio, and it can be concluded that the mechanism of the reaction of pyphy*a* formation is not affected in any of its steps by the type of oily matrix, so that the thermodynamic parameters characterized here can be extrapolated to any type of VOO matrix.

In the case of the reaction of 13^2-OH-phy*a* formation (**Figure 6**), the Arrhenius straight lines for matrices D and J (medium and low pigmentation) are close to each other and their intervals of confidence overlap, which make them isoenthalpic and isoentropic straight lines. Moreover, there is a cutoff point, or cutoff range, (enlarged in the figure) where these straight lines intersect with the Arrhenius straight line for matrix N (high pigmentation). This point (isokinetic temperature) is estimated as 324 ± 10 K (51 °C). These results are clearly consistent with the data for the increase in enthalpy ($\Delta H^{\#}$, **Table 4**), which show significant differences between samples D/J and N. In this case, there is an isokinetic ratio, and therefore the mechanism of the reaction of OH-phy*a* formation is affected, in one or another of its steps, by the type of matrix. Thus, at temperatures above the isokinetic, this reaction is quicker in the high-pigmentation matrices (oils at the start of the season), and below that temperature there will be predilection for medium- or low-pigmentation matrices. Therefore, a higher content of radical scavengers as tocopherol or carotenoids in VOO at the beginning of the harvesting season partly explains this result because these compounds can inhibit free radicals via the mechanism of formation of OH-phy*a*. In contrast, at temperatures higher than the isokinetic temperature, other components with prooxidant activity may counteract this effect; this reaction is more favored in the highly pigmented VOO.

Compensation Effect. Historically, the isokinetic ratio and the compensation effect have been considered to be synonymous. This is because there is sometimes a linear relationship between the logarithm of the pre-exponential factor and the activation energy, between the entropy and enthalpy of activation, or between the changes in enthalpy and entropy of a series of reactions with a common mechanism. However, Liu and Guo (*33*) have demonstrated that the compensation effect and the isokinetic effect are not necessarily synonymous and that the existence of one does not imply the existence of the other.

When the change of medium affects the reaction rate, in the sense of causing its increase, the corresponding parameters of activation are reduced. This effect has been defined as the law of compensation (*34*), and its equation is

$$\Delta H^{\ddagger}_{i} = \Delta H^{\ddagger}_{0} - \beta \Delta S^{\ddagger} \qquad (12)$$

where $\Delta H^{\ddagger}_{0}$ is the ordinate at the origin, without a physical sense, and β is the slope of the straight line determined in the plane $\Delta H^{\ddagger}$ versus $\Delta S^{\ddagger}$.

Table 5. Isokinetic Temperature (T_{isok}) and Determination Coefficients (R^2) Estimated by Leffer's Compensation Law ($\Delta H^{\ddagger}_i = \Delta H^{\ddagger}_0 + \beta\Delta S^{\ddagger}$) for the Thermal Degradation Reactions of Chlorophyll Compounds of Series *a* in Virgin Olive Oil

reaction[a]	β[b]	SE	R^2
D. phy*a*	310.10*[c]	43.05	0.98
F. pyphy*a*	361.62	55.93	0.98
F. OH-phy*a*	328.61*	16.92	0.99
F. lac-phy*a*	338.84	30.90	0.99
D. pyphy*a*	359.52	28.31	0.99
D. OH-phy*a*	342.21*	4.62	0.99
D. lac-phy*a*	407.60	227.31	0.73

[a] Reactions according to the kinetic mechanism shown in **Figure 3**; D, degradation; F, formation; phy, pheophytin; pyphy, pyropheophytin; OH-phy, 13^2-OH-pheophytin; lac-phy, 15^1-OH-lactone-pheophytin; [b] $\beta = T_{isok}$; [c] * indicates significant differences ($p < 0.05$) with the mean harmonic temperature (T_{hm}) = 362 K.

However, when β has the dimension of temperature, this is defined as isokinetic temperature (T_{iso}), expressed in Kelvin (K), and the behavior is denominated the isokinetic effect because at that temperature the rate constant of all the reactions complies with the equation

$$\Delta G_i(\beta) = \Delta H_i - \beta\Delta S_i = \alpha \quad (13)$$

where ΔG is the increase in Gibbs free energy, ΔH is the increase in enthalpy, ΔS is the increase in entropy, and α is a constant.

In other words, there is a common point of intersection of the Arrhenius (or van't Hoff) straight lines that describe the kinetics of a series of similar reactions. The value of β is distant from the experimental temperature range of most of the cases reported in the bibliography and is greater than the mean experimental temperature.

Exner (*35*) suggested using the regression in the plane ΔH versus ΔG as a statistical method to examine the enthalpy−entropy relationship. However, the compensation effect can occur, with ΔG being approximately constant within a series of reactions whenever ΔH and ΔS vary significantly. This approach to defining the compensation effect is based on the assumption that the data for the correlation are error-free. In experimental works, however, errors are inevitable, and the data used are, therefore, estimators of the corresponding variables. Consequently, it is possible that the real values are not correlated, although their estimators are. This would be the case in the so-called false compensation effect or false compensation. For example, if the experimental errors in ΔG are smaller than the errors in ΔH, the regressions in the plane ΔH versus ΔS are difficult to interpret.

The problems posed by experimental errors, on the one hand, and the interpretation of the plane ΔH versus ΔG, on the other, led Krug et al. (*36*) to propose that the straight line in the plane ΔH versus ΔS is only a manifestation of the statistical pattern of the compensation, and this hypothesis can be ruled out if the estimation of the slope is sufficiently different from the harmonic temperature (T_{hm}), defined as

$$T_{hm} = \frac{n}{\sum_{i=1}^{n} \frac{1}{T_i}} \quad (14)$$

Recently, Rudra et al. (*37*) found a linear relationship between enthalpy and entropy for chlorophylls *a* and *b* and their total degradation in thermally processed coriander puree at pH 4.5−8.5 ($R^2 = 0.99$), but did not indicate a true thermodynamic compensation effect ($T_\beta \approx T_{hm}$).

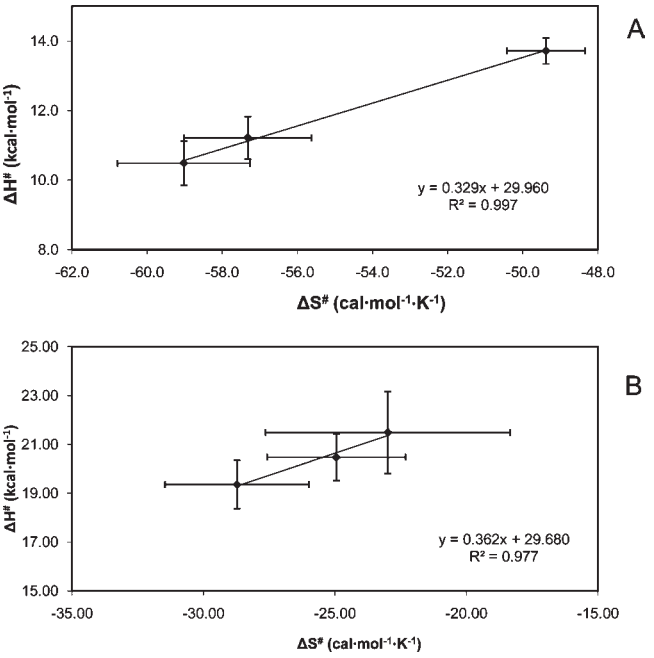

Figure 7. Graphic representation of $A\Delta H^{\ddagger}$ versus $A\Delta S^{\ddagger}$ by error bars method (*33*): (**A**) true compensation effect for the formation of 13^2-OH-pheophytin *a*; (**B**) false compensation effect for the formation of pyropheophytin *a* in VOO samples.

Liu and Guo (*33*) have proposed a method for distinguishing the real compensation effects from the false ones, based on a graphical representation of the experimental values of enthalpies and entropies with their error bars in the plane $\Delta H^{\ddagger}$ versus $\Delta S^{\ddagger}$.

To apply this study to our experimental data the linear regressions $A\Delta H^{\ddagger}$ versus $A\Delta S^{\ddagger}$ have been estimated for each of the reactions comprising the mechanism of phy*a* degradation. **Table 5** shows the values obtained for the slope β and the corresponding determination coefficients (R^2). It can be observed that the good coefficients of correlation obtained ($R^2 > 0.97$) (except in the degradation of lac-phy*a*) indicate the existence of a compensation effect between $A\Delta H^{\ddagger}$ and $A\Delta S^{\ddagger}$. However, from the comparison between the estimated isokinetic temperature (β) and the T_{hm} under the study conditions (362 K), it is deduced that this compensation effect can be real only for the degradation of phy*a*, the formation of OH-phy*a*, and the degradation of OH-phy*a*, for which the differences between the temperatures are significant. Finally, application of the method of error bars proposed by Liu and Guo (*33*) shows that of all the reactions, only the reaction of OH-phy*a* formation shows a real compensation effect (**Figure 7**), which moreover is limited, as the entropic and enthalpic values for the low- and medium-pigmentation matrices do not present significant differences.

The analysis of the reaction intermediaries that appear during the thermodegradation of pheophytin *a* to colorless products in VOO has established that the degradative process is not simple, but takes place in several competitive elemental steps. A marked effect of temperature on the reaction mechanism was revealed, whereas the effect of the medium was only partially significant in one of the steps: the formation reaction of 13^2-OH-pheophytin, the free radical mechanism of which could be influenced by the content in radical scavengers.

This study has yielded a mathematical model that predicts the formation of pyropheophytin *a* in VOO with time and depending on temperature. Work is currently being conducted to validate it. The study is carried out with VOOs stored at room temperature.

ACKNOWLEDGMENT

We thank Sergio Alcañiz-García for his technical assistance.

LITERATURE CITED

(1) Mínguez-Mosquera, M. I.; Gandul-Rojas, B.; Gallardo-Guerrero, M. L.; Roca, M.; Jarén-Galán, M. Chlorophylls. In *Methods of Analysis in Funtional Foods and Added Nutraceuticals*, 2nd ed.; Hurst, W. J., Ed.; CRC Press: Boca Raton, FL, 2007; Chapter 7, pp 337−400.

(2) Ferruzzi, M. G.; Blakeslee, J. Digestion, absorption, and cancer preventive activity of dietary chlorophyll derivatives. *Nutr. Res. (N.Y.)* **2007**, *27*, 1–12.

(3) Gandul-Rojas, B.; Roca-L. Cepero, M.; Mínguez-Mosquera, M. I. Use of chlorophyll and carotenoid pigment composition to determine authenticity of virgin olive oil. *J. Am. Oil. Chem. Soc.* **2000**, *77*, 853–858.

(4) Mínguez-Mosquera, M. I.; Gandul-Rojas, B.; Garrido-Fernández, J.; Gallardo Guerrero, L. Pigment presence in virgin olive oil. *J. Am. Oil Chem. Soc.* **1990**, *67*, 192–196.

(5) Ward, K.; Scarth, R.; Daun, J. K.; Thorsteinson, C. T. Effects of processing and storage on chlorophyll derivatives in commercially extracted canola oil. *J. Am. Oil Chem. Soc.* **1994**, *71*, 811–815.

(6) Gandul-Rojas, B.; Mínguez-Mosquera, M. I. Chlorophyll and carotenoid composition in virgin olive oils from various Spanish olive varieties. *J. Sci. Food Agric.* **1996**, *72*, 31–39.

(7) Psomiadou, E.; Tsimidou, M. Stability of virgin olive oil. 2 Photooxidation studies. *J. Agric. Food Chem.* **2002**, *50*, 722–727.

(8) Gallardo Guerrero, L.; Roca, M.; Gandul-Rojas, B.; Mínguez Mosquera, M. I. Effect of storage on the original pigment profile of Spanish virgin olive oil. *J. Am. Oil Chem. Soc.* **2005**, *82*, 33–39.

(9) Gandul-Rojas, B.; Roca, M.; Mínguez-Mosquera, M. I. Chlorophyll and carotenoid pattern in virgin olive oil. Adulteration control. In *Proceeding of the 1st International Congress on Pigments in Food Technology (PFI)*, PFT Press: Seville, Spain; Mínguez-Mosquera, M. I., Jarén-Galán, M., Hornero-Méndez, H., Eds.; 1999; pp 381−386, PFI: ISBN 8469901850.

(10) Serani, A.; Piacenti, D. Sistema analitico per l'identificazione di oli deodorati in oli vergini di oliva. Nota 1 − Analisi dei pigmento clorofilliani in oli vergini di oliva. *Riv. Ital. Sostanze Grasse* **2001**, *78*, 459–463.

(11) Anniva, C.; Grigoriadou, D.; Psomiadou, E.; Tsimidou, M. Z. Pheophytin α degradation products as useful indices in the quality control of virgin olive oil. *J. Am. Oil Chem. Soc.* **2006**, *83*, 371–375.

(12) The International Olive Council (IOC) Trade Standard applying to Olive Oil and Olive-Pomace Oil. International Olive Council Website, www.internationaloliveoil.org, 2006; COI/T.15/NC n°3/Rev. 2.

(13) Watanabe, T.; Hongu, A.; Honda, K.; Nakazato, M.; Konno, M.; Saithoh, S. Preparation of chlorophylls and pheophytins by isocratic liquid chromatography. *Anal. Chem.* **1984**, *56*, 251–256.

(14) Hynninen, P. H. Chemistry of chlorophyll modifications. In *Chlorophylls*; Scheer, H., Ed.; CRC Press: Boca Raton, FL, 1991; pp 145−210.

(15) Mínguez-Mosquera, M. I.; Gandul-Rojas, B. High-performance liquid chromatographic study of alkaline treatment of chlorophyll. *J. Chromatogr.* **1995**, *690*, 161–176.

(16) Walalí-Loudiyi, D.; Chimitah, M.; Loussert, R.; Mahhou, A.; Boulouha, B. Morphologic and physiologic characters of olive chlones from Picholine Marroqui variety. *Olivae* **1984**, *3*, 26–31.

(17) Mínguez-Mosquera, M. I.; Gandul-Rojas, B.; Gallardo-Guerrero, L. Rapid method of quantification of chlorophylls and carotenoids in virgin olive oil by HPLC. *J. Agric. Food Chem.* **1992**, *40*, 60–63.

(18) Hornero-Méndez, D.; Gandul-Rojas, B.; Mínguez-Mosquera, M. I. Routine and sensitive SPE-HPLC method for quantitative determination of pheophytin *a* and pyropheophytin *a* in olive oils. *Food Res. Int.* **2005**, *38*, 1067–1072.

(19) Van Boekel, M. A. J. S. Kinetic modeling of food quality: a critical review. *Compr. Rev. Food Sci. Food Saf.* **2008**, *7*, 144–158.

(20) Brown, M. B.; Forsythe, A. B. Robust tests for the equality of variances. *J. Am. Stat. Assoc.* **1974**, *69*, 364–367.

(21) Marangoni, A. G. Kinetic model for chlorophyll degradation in green tissue. 2. Pheophorbide degradation to colorless compounds. *J. Agric. Food Chem.* **1996**, *44*, 3735–3740.

(22) Hörtensteiner, S. Chlorophyll degradation during senescence. *Annu. Rev. Plant Biol.* **2006**, *57*, 55–77.

(23) Mínguez-Mosquera, M. I.; Gandul-Rojas, B.; Gallardo-Guerrero, M. L. Mechanism and kinetics of the degradation of chlorophylls during the processing of green table olives. *J. Agric. Food Chem.* **1994**, *42*, 1089–1095.

(24) Heaton, J. W.; Lencki, R. W.; Marangoni, A. G. Kinetic model for chlorophyll degradation in green tissue. *J. Agric. Food Chem.* **1996**, *44*, 399–402.

(25) Canjura, F. L.; Schwartz, S. J.; Nunes, R. V. Degradation kinetics of chlorophylls and chlorophyllides. *J. Food Sci.* **1991**, *56*, 1639–1643.

(26) Weemaes, C. A; Ooms, V.; Van Loey, A. M.; Hendrickx, M. E. Kinetics of chlorophyll degradation and color loss in heated broccoli juice. *J. Agric. Food Chem.* **1999**, *47*, 2404–2409.

(27) Pérez-Galvéz, A.; Jarén-Galán, M.; Mínguez-Mosquera, M. I. Effect of high-temperature degradative processes on ketocarotenoids present in paprica oleoresins. *J. Agric. Food Chem.* **2000**, *48*, 2966–2971.

(28) Psomiadou, E.; Tsimidou, M. Stability of virgin olive oil. 1. Autoxidation studies. *J. Agric. Food Chem.* **2002**, *50*, 716–721.

(29) Gupta, M. C.; Viswanath, S. G. Kinetics compensation effect in thermal degradation of polymers. *J. Therm. Anal.* **1996**, *47*, 1081–1091.

(30) Galwey, A. K.; Brown, M. E. Arrhenius parameters and compensation behavior in solid-state decomposition. *Thermochim. Acta* **1997**, *300*, 107–115.

(31) Boots, H. M. J.; de Bokx, P. K. The compensating-mixture model for multicomponent systems and its application to ion exchange. *J. Phys. Chem.* **1990**, *94*, 6489–6495.

(32) Karpinski, Z.; Larsson, R. On the isokinetic effect of neopentane hydrogenolysis over metal catalysts. *J. Catal.* **1997**, *168*, 532–537.

(33) Liu, L.; Guo, Q. X. Isokinetic relationship, isoequilibrium relationship, and enthalpy−entropy compensation. *Chem. Rev.* **2001**, *101*, 673–695.

(34) Leffler, J. E. The enthalpy−entropy relationship and its implications for organic chemistry. *J. Org. Chem.* **1955**, *20* (9), 1202–1231.

(35) Exner, O. Statistics of enthalpy−entropy relationship 3. Processing of calorimetric data. *Collect. Czech. Chem. Commum.* **1973**, *38*, 799–812.

(36) Krug, R. R.; Hunter, W. G.; Grieger, R. A. Enthalpy−entropy compensation: 1. Some fundamental statistical problems associated with the analysis of Van't Hoff and Arrenhius data. 2. Separation of the chemical from the statistical effect. *J. Phys. Chem.* **1976**, *80*, 2335–2351.

(37) Rudra, S. G.; Sarkar, B. C.; Shivhare, U. S. Thermal degradation kinetics of chlorophyll in pureed coriander leaves. *Food Bioprocess Technol.* **2008**, *1*, 91–99.

Received for review December 11, 2009. Revised manuscript received March 31, 2010. Accepted April 20, 2010. This work was supported by the Comisión Interministerial de Ciencia y Tecnología (CICYT-EU, Spanish and European Government) and FEDER (CE) in the Project AGL 2004-07623-C03-02 and by the Junta de Andalucía (AGR 148-2005-6).